Available online at www.sciencedirect.com
SCIENCE DIRECT®
International Journal of Heat and Mass Transfer 49 (2006) 4444–4453
International Journal of HEAT and MASS TRANSFER
www.elsevier.com/locate/ijhmt

Synchronization of self-sustained thermostatic oscillations in a thermal-hydraulic network

Weihua Cai, Mihir Sen *, K.T. Yang, Rodney L. McClain

Hydronics Laboratory, Department of Aerospace and Mechanical Engineering, University of Notre Dame, Notre Dame, IN 46556, United States

Received 14 December 2005; received in revised form 22 April 2006
Available online 7 July 2006

Abstract

Flow and temperature oscillations occur under normal conditions in a thermal system with thermostatic control. We present experimental results of the synchronization of multiple oscillators in the secondaries of a thermal-hydraulic network. The test facility is composed of three secondary loops with heat exchangers that exchange heat with a primary heating loop on one side and a primary cooling loop on the other. A thermostatic controller senses the temperature at the outlet of a heat exchanger and modulates the flow rate in that loop. The flow valve is partially closed if the temperature goes above an upper limit and is completely opened if it falls below a lower limit. As a consequence a self-sustained flow and temperature oscillation is set up in that secondary. The frequency of the oscillation depends on the dead-band between the upper and lower temperature limits. Coupled oscillators are set up by the simultaneous action of multiple controllers on different branches. Frequency locking, phase synchronization as well as phase slips are observed to occur due to thermal-hydraulic coupling between the controllers. The phenomenon is a function of the detuning between them which is altered by changing the dead-band of the controllers.

Keywords: Thermal-hydraulic network; Oscillator; Synchronization; Thermostatic control

1. Introduction

Self-sustained oscillators are those that do not need external forcing to develop oscillations. Over the past decades, synchronization in a population of weakly coupled oscillators has attracted wide-spread interest among scientists in different fields. In 1958, when studying the alpha rhythm of brain waves, Wiener [1] suggested that "in the brain we have some sort of oscillators, and that these oscillators in some sense constitute a more accurate oscillator *en masse* than they do singly". Winfree [2], working within the framework of a mean-field model, pointed out that when a certain threshold is crossed, coupled oscillators may begin to synchronize spontaneously. An early theoretical explanation came from Kuramoto [3], who analyzed a mean-field model of a population of phase oscillators. This model is simple enough to be mathematically tractable and has since been further explored [4,5]. Synchronization is now understood to be a ubiquitous phenomenon [6–8], and has been observed and studied in many different kinds of natural and artificial systems. There are examples in biological [9–14], chemical [15–17], mechanical [18–21], fluid [22] and electrical [23–25] systems, among others. Some of the systems exhibit chaos [26–35] or are of fractional order [36].

Although synchronization of coupled self-sustained oscillators has attracted considerable attention in many other complex systems, there are no similar studies in the literature on thermal-hydraulic networks. In these systems, oscillation of flow or temperature may occur due to instabilities, periodic external disturbances, or changes in operating condition, among other factors. In addition, feedback control systems, with which we are concerned, are an important class of systems that may oscillate. Here we

* Corresponding author. Tel.: +1 574 631 5975; fax: +1 574 631 8341.
E-mail address: mihir.sen.1@nd.edu (M. Sen).

0017-9310/$ - see front matter © 2006 Elsevier Ltd. All rights reserved.
doi:10.1016/j.ijheatmasstransfer.2006.04.027

Nomenclature

A	amplitude
A, B, C	secondary loops
P_1, P_2	pumps
s	analytic signal
t	time (s)
T	temperature (°C)
T_u	thermostat upper temperature limit (°C)
T_l	thermostat lower temperature limit (°C)
T_s	thermostat set point (°C)
ΔT	thermostat temperature dead-band (°C)
V_i^j	valve in loop i with j indicating heating (h) or cooling (c)

Greek symbols

θ	phase angle (rad)
ϕ	phase difference (rad)
ω	frequency of oscillation without coupling (rad/s)
$\Delta\omega$	difference between ω's of two oscillators (rad/s)
Ω	frequency of oscillation with coupling (rad/s)
$\Delta\Omega$	difference between Ω's of two oscillators (rad/s)

Superscripts

c	cooling side
h	heating side

Other symbols

$\widehat{\ }$	Hilbert transform
$\langle\rangle$	temporal mean

use the specific example of thermostatic control of temperature which, even in normal operation, has a self-sustained oscillatory behavior. Interaction between oscillations in diverse parts of a network due to independently acting thermostats is of concern in the design of large-scale thermal control systems as, for example, in heating and cooling systems in a large office building; the temperature in individual offices may be thermostatically controlled, but it is not correct to assume that the resulting dynamics of each of the rooms are independent of each other.

In general, thermal-hydraulic networks consist of heat exchangers, piping and pumps, and are widely used in building HVAC systems, in power plants and in the processing industry. Though the performance of the individual components of a network is fairly well understood, the interaction between them when put together has received less attention. Coupling of sub-systems through fluid flow and heat transfer influences the operation of the system as a whole. There are many simulations of the dynamics of thermal-hydraulic systems, such as in nuclear power plants [37]. Thermostats are very common in industrial and building thermal control applications [38,39], and some authors have specifically looked at the modeling of system behavior due to thermostats. This has included whole building energy simulations [40], hot-water heaters [41], household refrigerators [42], engine cooling [43,44], variable-air-volume air conditioning [45], radiant floor heating [46], automotive thermostats [47], thermostatically controlled appliances [48] and the energy performance of coupled-control units [49].

In the present work, we look at oscillations due to multiple thermostatic controllers located on different loops of a thermal-hydraulic network. There is dynamic coupling between the loops, and this leads to the observation of synchronization under certain conditions. The work was carried out in an experimental facility that has previously been used for studies of control strategies and network dynamics [50–52], as well as steady-state interactions of the pressure, flow rate and temperature between secondary loops [53].

2. Experimental procedure

2.1. Facility

A simplified diagram of the experimental facility is shown in Fig. 1, details of which are given elsewhere [50–53]. There are two primaries: one is a hot-water loop (the water is heated by heaters HT_1 and HT_2 with the temperature maintained at 37.8 °C) driven by pump P_1, and the other is cold-water (cooled by heat exchanger HX_m connected to the building chilled-water line) driven by P_2. Between them there are three secondaries, A, B and C, on which there are

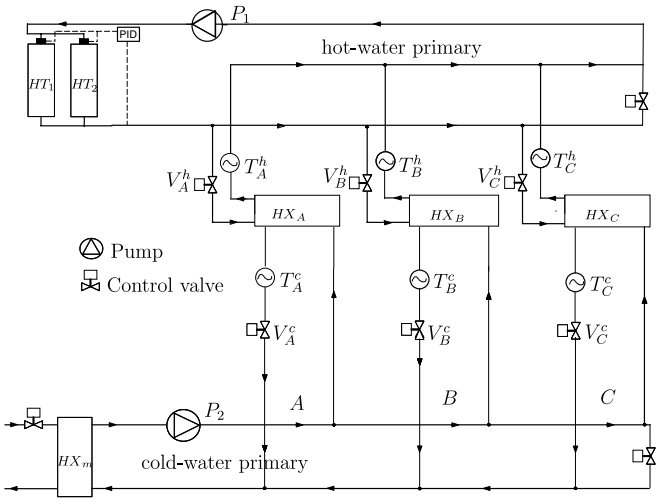

Fig. 1. Layout of network.

heat exchangers HX_A, HX_B and HX_C, exchanging heat with the two primaries. There are computer-controlled, pneumatically-actuated, two-way valves on the heating (V_A^h, V_B^h and V_C^h) and cooling (V_A^c, V_B^c and V_C^c) sides of each heat exchanger to control the flow rate. Control valves on the heating side are located upstream of the heat exchangers, and due to the space limitations those on the cooling side are downstream. The location of valves, pumps and other components were not optimized. Water temperatures are measured by type J ungrounded thermocouples at both the heating (T_A^h, T_B^h and T_C^h) and cooling (T_A^c, T_B^c and T_C^c) side outlets of each heat exchanger. The time constant of the thermocouple probe, which is around 0.55 s, is much smaller than the time scales in the experiment. Data acquisition, processing and control are carried out by a PC running LabVIEW.

2.2. Signal analysis

Compared to analytical or numerical data, it is harder in experiments to analyze almost-periodic events and to determine instantaneous phase and frequency from data. Here we use some of the techniques of time–frequency analysis of non-stationary signals [54], as is commonly done in phase-synchronization studies [15,27], to determine instantaneous values of amplitudes, phases and frequencies for the temperature signals. The computations were done in MATLAB.

We take the deviation of the temperature from the mean as $T'(t) = T(t) - \langle T\rangle$, where $\langle\ \ \rangle$ is a temporal mean defined by

$$\langle T\rangle = \lim_{\tau\to\infty}\frac{1}{\tau}\int_0^\tau T(t)\mathrm{d}t. \tag{1}$$

Applying the Hilbert transform

$$\widehat{T}'(t) = \frac{1}{\pi}\mathrm{PV}\int_{-\infty}^{\infty}\frac{T'(t)}{t-\tau}\mathrm{d}\tau, \tag{2}$$

where PV is the Cauchy principal value, we can obtain the so-called complex *analytic signal* $s(t) = T'(t) + \mathrm{i}\widehat{T}'(t)$, where $\mathrm{i} = \sqrt{-1}$. This can be written in terms of an instantaneous amplitude $A(t)$ and phase $\theta(t)$ as $s(t) = A(t)\mathrm{e}^{\mathrm{i}\theta(t)}$, where $A(t) = (T'^2 + \widehat{T}'^2)^{1/2}$ and $\theta(t) = \tan^{-1}(\widehat{T}'/T')$. Numerical differentiation [55,56] of the instantaneous phase is applied to determine the instantaneous frequency so that $\omega = \mathrm{d}\theta/\mathrm{d}t$.

2.3. Thermostatic self-sustained oscillations

The three controllers reside in the PC in the form of software. For each controller the sensor is a thermocouple at one of the outlets of a heat exchanger and the actuator is a two-way valve at the same location. Actuation of the valve is dependent on the temperature signal. The temperature control method used here is *thermostatic* (also called *on–off, two position* or *bang–bang*). If the water temperature T rises above an upper limit T_u, the controller shuts the valve partially (it is not shut completely so as to allow a small flow whose temperature can be measured). If, on the other hand, the temperature falls below the lower limit T_l, the valve is completely opened. $\Delta T = T_u - T_l$ is defined as the dead-band, and the set point of the controller can be considered to be the mean $T_s = (T_u + T_l)/2$. The temperature and flow rate oscillate in time as a result of thermostatic control.

To produce a single uncoupled oscillator, a thermostatic controller is used on, for example, the temperature T_B^c on the cooling side of the heat exchanger HX_B as sensor and the valve V_B^c as actuator. Temperature measurements are recorded long enough until they become more or less periodic, which it does after a few seconds. To reduce the random noise in the temperature signal, 500 data points per second were taken and the averaged result was used. A typical oscillation of the temperature T_B^c is shown in Fig. 2. The period is around 20 s in this example. The form of each period is not exactly sinusoidal: it takes longer for the temperature to rise than to fall. Nor are the periods all exactly identical. The T_u and T_l limits used by the controller are also indicated in the figure, and it can be seen that the temperature over- and under-shoots the limits. The exact form of the temperature–time relation depends on the network configuration and parameters. Temperatures at other locations within the network also oscillate at the same frequency due to interaction with this controller and driven by it.

The mean frequency of oscillation $\langle\omega\rangle$ is defined in a manner similar to Eq. (1), and is obtained from the instantaneous frequency $\omega(t)$ by numerical integration. Since the measured temperature is not exactly periodic, the interval τ is taken sufficiently large so that the integral becomes independent of it. As shown in Fig. 3, $\tau \approx 500$ s appears to be sufficient. The mean frequency is a function of the dead-band with a complicated dependence on the network characteristics. In general, however, as the dead-band ΔT for thermostatic action is increased, it takes longer for the

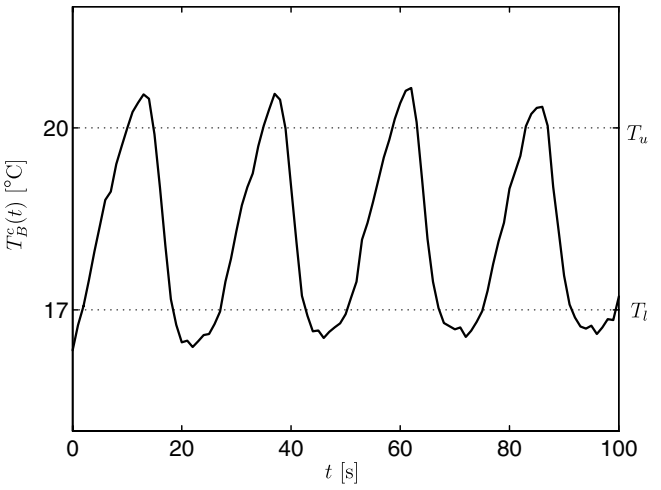

Fig. 2. Typical oscillation of the temperature T_B^c. The upper and lower limits of thermostatic control are indicated.

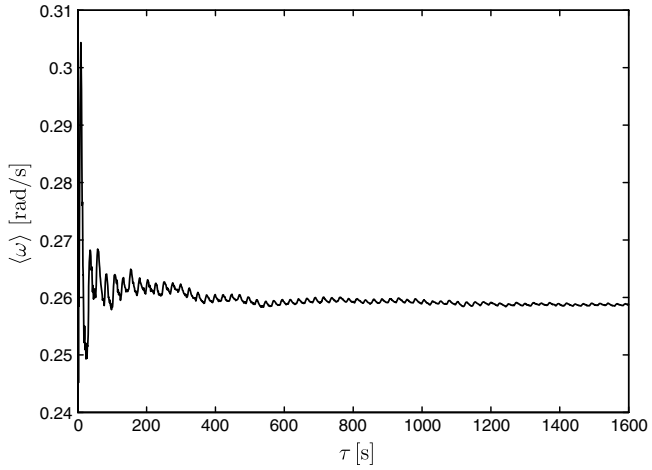

Fig. 3. Effect on averaging of interval of integration τ.

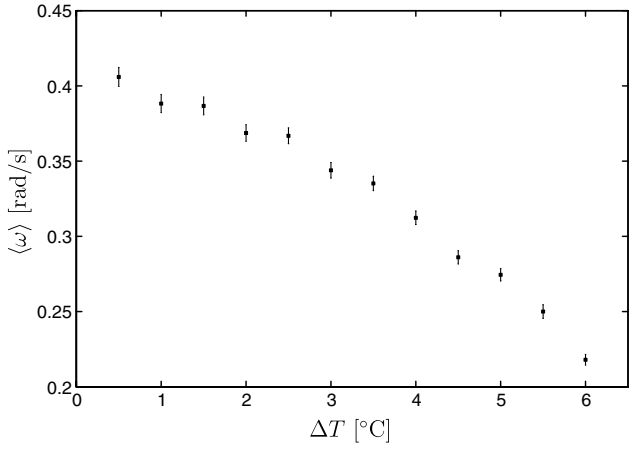

Fig. 4. Effect of dead-band on frequency of T_B^c.

temperature to go from one to the other and back again, and the period of the oscillation consequently increases. This is shown in Fig. 4 which is a result of measuring $\langle\omega\rangle$ for different ΔT. This indicates that the frequency of the thermostatic oscillator can be changed by altering the dead-band, a fact that we will use to detune multiple controllers.

2.4. Multiple controllers

The experimental facility has three secondary loops that are nominally identical. Thermostatic control can be applied to a temperature and actuator pair in more than one loop. Since there are three heat exchangers, there are six outlets where the temperature can be sensed and the valve actuated. These locations are marked in Fig. 1 as $(T_A^h, V_A^h), (T_B^h, V_B^h), (T_C^h, V_C^h)$ for the heating sides, and $(T_A^c, V_A^c), (T_B^c, V_B^c)$ and (T_C^c, V_C^c) for the cooling sides. Each location, if used as a controller, provides a potential oscillator.

When more than one oscillator is in operation, the frequency of each may be different than if it were operating

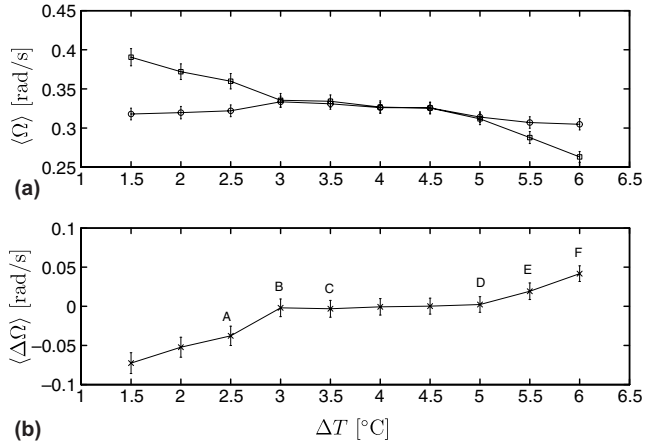

Fig. 5. Coupled (a) frequencies of temperatures T_B^c (squares) and T_C^c (circles) and (b) frequency difference. Points A–F correspond to curves in Fig. 6.

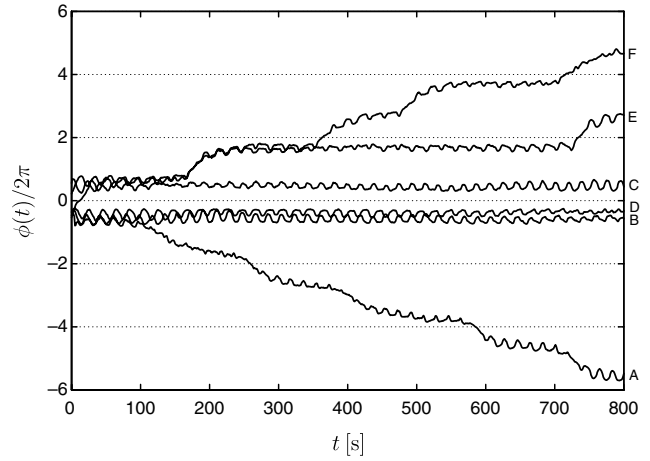

Fig. 6. Phase difference between temperatures T_B^c and T_C^c. Curves A–F correspond to points in Fig. 5.

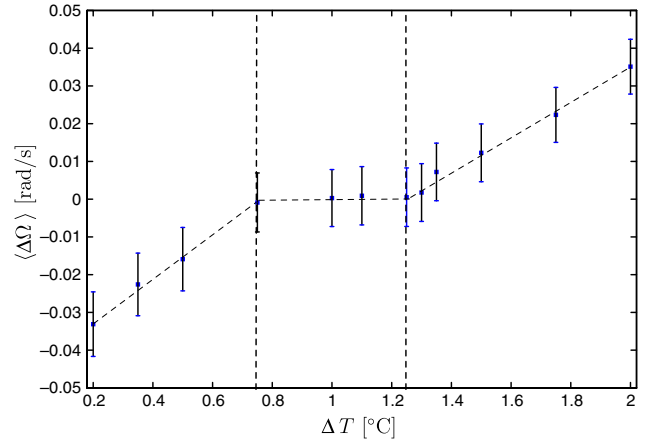

Fig. 7. Difference in coupled frequencies for different dead-bands. Synchrony is exhibited in interval between vertical dashed lines.

alone. We will use the symbol ω as before to denote the uncoupled frequency of an oscillator when it is the only one in operation, and use Ω for its coupled frequency when another oscillator is also simultaneously functioning. In general, the two will be different because of interaction between the oscillators.

Generally speaking, there are two possible parameters to change during the study of the collective dynamics of

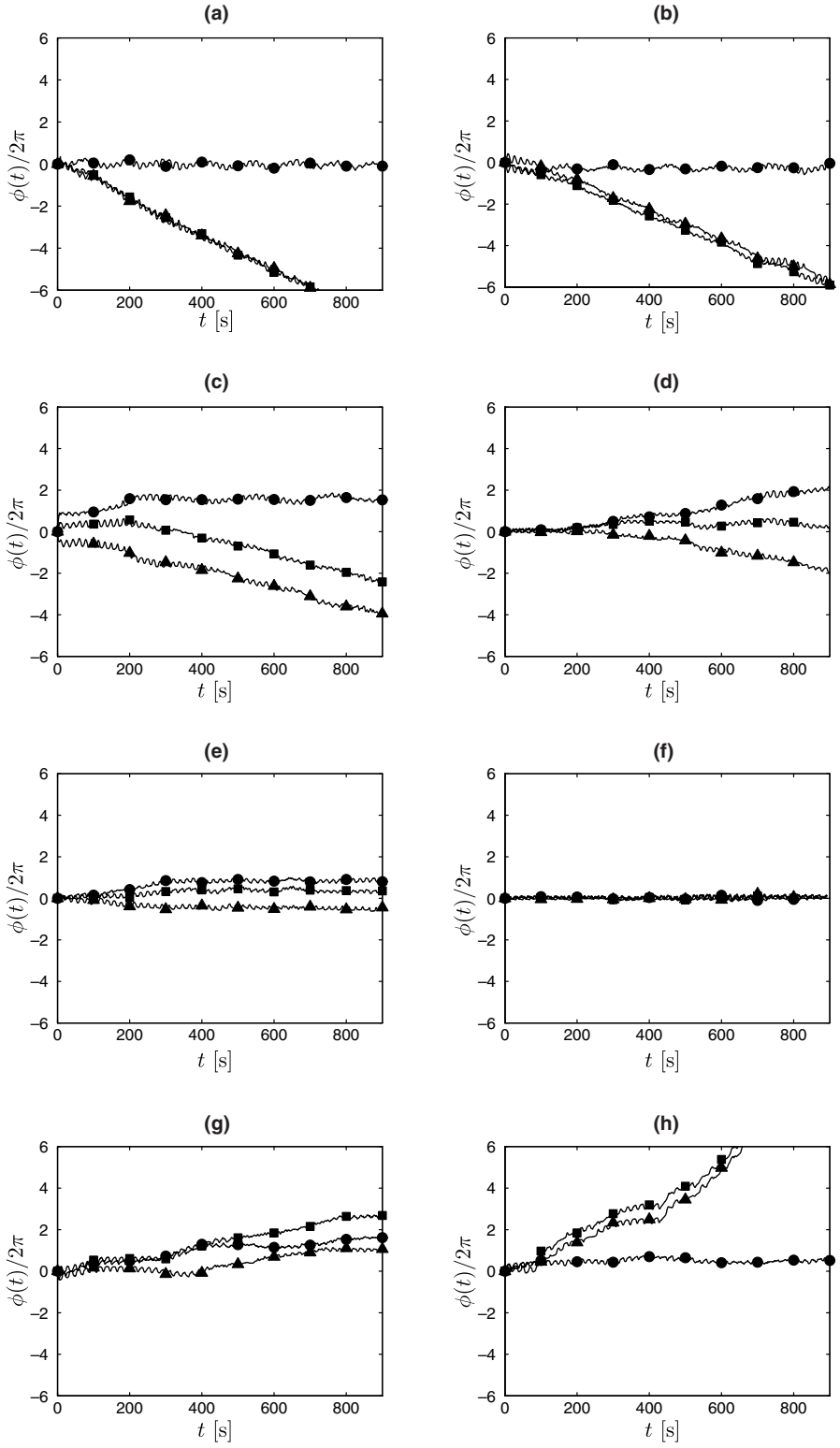

Fig. 8. Phase differences between temperatures T_A^c, T_B^c and T_C^c with variation of dead-band of T_C^c. Circles, squares and triangles correspond to ϕ_{AB}, ϕ_{AC} and ϕ_{BC}, respectively. $\Delta T =$ (a) 0.5 °C, (b) 1.0 °C, (c) 1.5 °C, (d) 2.0 °C, (e) 2.5 °C, (f) 3.0 °C, (g) 3.5 °C and (h) 4.0 °C.

coupled oscillators. The first is the physical coupling between the oscillators, and the second is the detuning (i.e. the difference in the uncoupled frequency ω of each). Since there is no way to change the coupling between the loops in the present case, we will use detuning as a parameter. This we will do by modifying the dead-band of the oscillators which will change their uncoupled frequency of oscillation. It can be done independently for each controller through the software. If ω_1 and ω_2 are the uncoupled frequencies of two oscillators, then $\Delta\omega = \omega_1 - \omega_2$ represents the *detuning* between them. Of course, $\Delta\Omega = \Omega_1 - \Omega_2$ is a different quantity that depends on the coupling between the oscillators. For completely decoupled oscillators, $\omega_1 = \Omega_1$ and $\omega_2 = \Omega_2$, and on the other hand, complete *frequency locking* between the two oscillators means that $\Delta\Omega = 0$ regardless of the value of $\Delta\omega$. Another manifestation of synchronization is *phase locking* [6,11] where the phase difference $\phi = \theta_1 - \theta_2$ is a constant.

3. Results and discussion

Steady-state interaction between the loops was previously measured [53] where it was shown that a change in flow rate in one secondary affected the pressure differences, flow rates and temperatures in the others also. The dynamics of coupling between the loops are complex, but some physical reasons can be put forth. If a valve in one secondary is closed slightly, some of the flow in the primary is momentarily diverted to the other secondaries which then affects the temperatures. There are different times scales associated with interactions between each one of the variables. In the present case, there are two opposing effects in operation. A decrease of the temperature in one loop is due to an increase in the flow rate in that loop; the flow rates in other loops will decrease causing the outlet temperature to increase. In this sense, the interaction is repulsive. However, a decrease of the temperature in one loop also reduces the water temperature in the primary and therefore the inlet temperature to the other loops. In this sense, the interaction between the oscillators is attractive. In addition, the other controllers are also actively trying to contain the temperature between the limits. It is not difficult to see why detuning can have an important effect on the response of the network. There is also coupling between the heating and cooling sides of a heat exchanger. This, however, is not hydrodynamic but thermal; temperatures on one side affect those on the other. Thus the coupling across the two sides can be expected to be weaker than that on the same side.

There are many combinations of multiple controllers that can be applied to the six water-outlet locations of the three heat exchangers, but we will not experiment with all. We will first select two controllers and then three. For each set of experiments, only the valves selected for control are varied in time, while all the others are fixed. Detuning is introduced by a series of dead-band changes in one controller and keeping the other controllers fixed.

3.1. Two controllers

Study of the dynamics of controllers located on the heating and cooling sides of the same heat exchanger is not very interesting since the coupling between them will be strong and does not address the issue of coupling between oscillators in different loops. Thus the controllers will be chosen to be on different heat exchangers, but with both on the cooling side or one each on either side.

3.1.1. Controllers at T_B^c and T_C^c

We first choose the locations T_B^c and T_C^c for two controllers on the cooling side. The controller for T_C^c is fixed at $T_s = 14\,^\circ\mathrm{C}$, $\Delta T = 4\,^\circ\mathrm{C}$, while that for T_B^c has $T_s = 14.5\,^\circ\mathrm{C}$ with a variable dead-band. Figs. 5(a) and (b) show the $\langle\Omega\rangle$ and $\langle\Delta\Omega\rangle$ responses of the network, respectively, for a number of different values of the dead-band ΔT. For small and large ΔT the two coupled frequencies

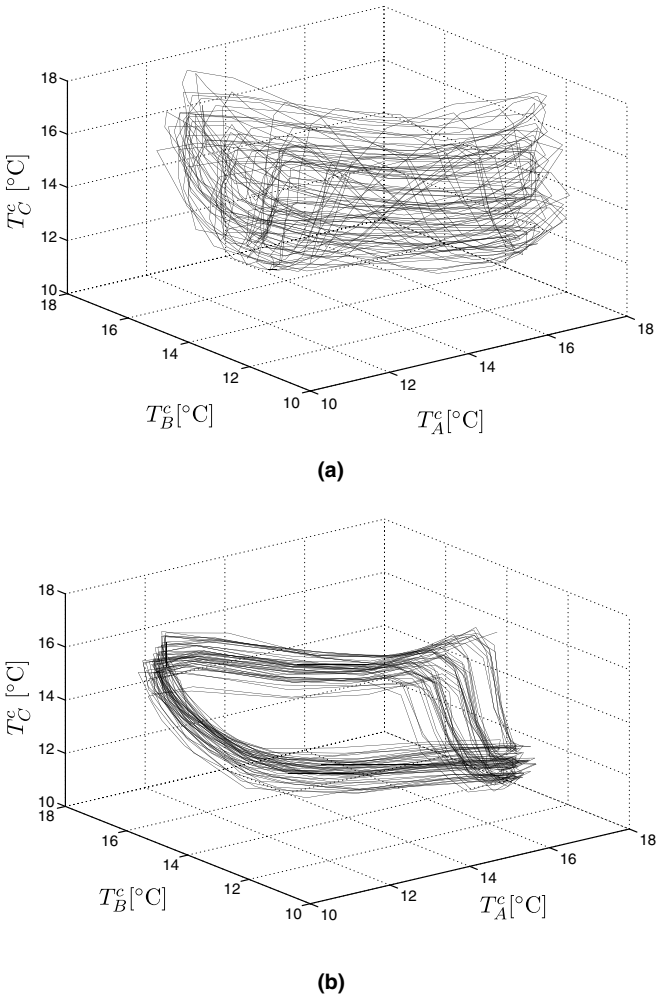

Fig. 9. Phase plot of temperatures T_A^c, T_B^c and T_C^c: $\Delta T = $ (a) 2.0 °C and (b) 3.0 °C.

change, while in the middle they are locked together in synchrony. (a) shows that in the unsynchronized regions, the $\langle\Omega\rangle$ vs. ΔT line is steeper for T_B^c, which is where the dead-band change is affected. However, the coupled frequency of T_C^c also changes, though not as much. The difference in the coupled frequency, $\langle\Delta\Omega\rangle$, in (b) shows

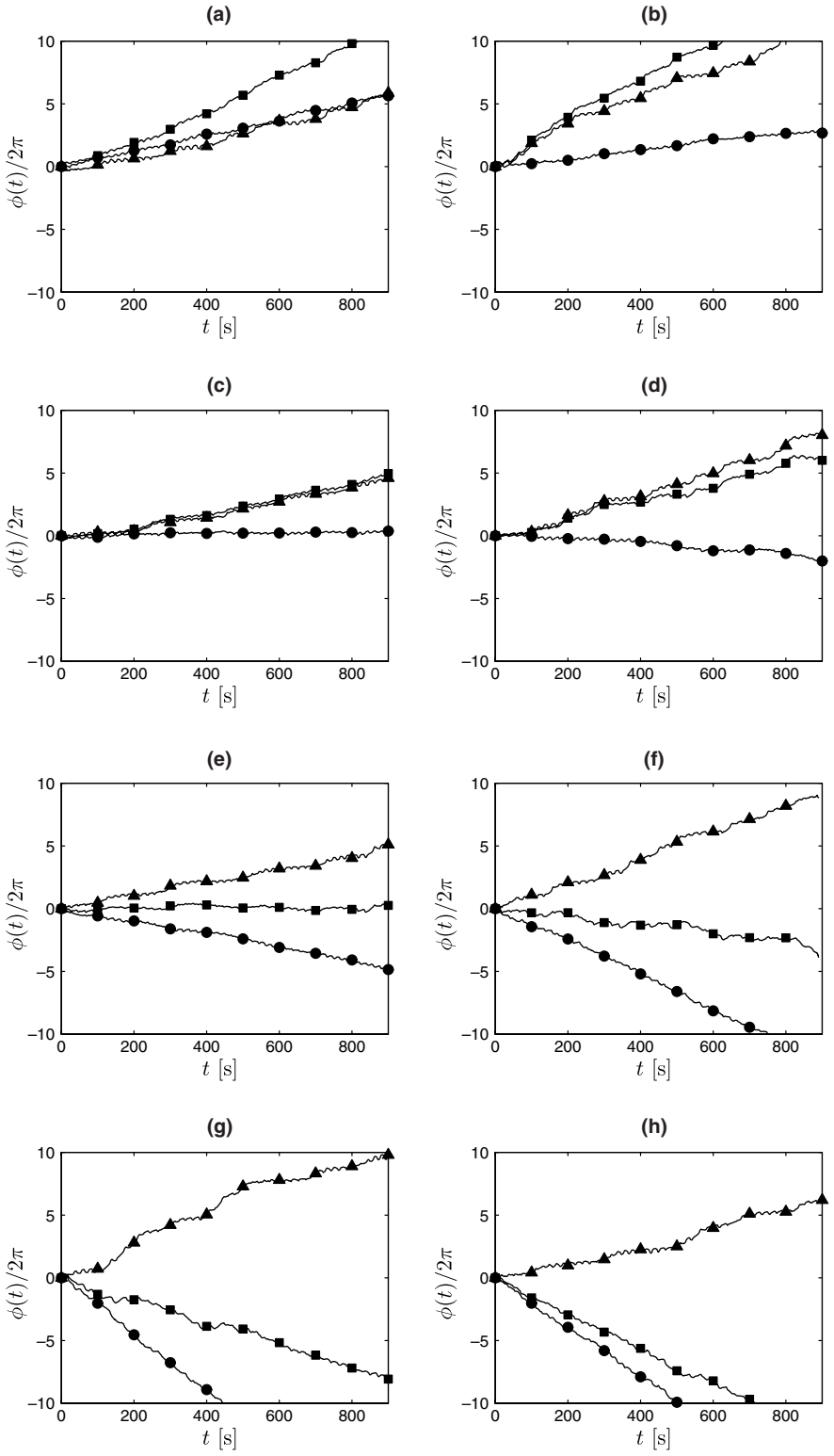

Fig. 10. Phase differences between temperatures T_A^h, T_B^c and T_C^c with variation of dead-band of T_A^h. Circles, squares and triangles correspond to ϕ_{AB}, ϕ_{AC} and ϕ_{BC} respectively. $\Delta T =$ (a) 0.5 °C, (b) 1.0 °C, (c) 1.5 °C, (d) 2.0 °C, (e) 2.5 °C, (f) 3.0 °C, (g) 3.5 °C and (h) 4.0 °C.

the same phenomenon slightly differently. For the dead-band in the range 3.0 °C < ΔT < 5.0 °C there is a plateau where $\langle \Delta\Omega \rangle$ is almost zero indicating synchronization. Outside this region the two oscillators are out of synchrony.

The phase difference $\phi(t)$ is shown for six different values of the dead-band in Fig. 6 (letters A–F refer to corresponding points on Fig. 5(b)). In curves A and F at the two extremes, $|\phi|$ grows indefinitely: the oscillators are out of synchrony. In curve E the growth is not uniform. There are times when $|\phi|$ is nearly constant while at times it changes rapidly by 2π (a phenomenon that is often known as phase slip [6]). It is an indication of transition to synchronization. In curves B, C and D, however, $|\phi|$ is a constant throughout implying that the two oscillators are phase-synchronized.

3.1.2. Controllers at T_A^h and T_C^c

We now choose one controller on the heating and one on the cooling sides, for example, T_A^{h} and T_C^{c}. Again, frequency detuning is achieved by changing the dead-band of T_A^{h} with $T_{\mathrm{s}} = 21.5$ °C while that of T_C^{c}, with $T_{\mathrm{s}} = 14$ °C and $\Delta T = 4$ °C, is kept constant. $\langle \Delta\Omega \rangle$ vs. ΔT is plotted in Fig. 7, where a plateau exists between the dashed vertical lines indicating synchronization there. The dead-band interval in which this happens is about 0.5 °C wide, being much smaller than the 2 °C in Section 3.1.1 where the two controllers were on the same side.

3.2. Three controllers

The collective behavior of three active controllers is more complex. In one experiment we will choose all three on the cooling side, and in the other choose two on the cooling and one on the heating side.

3.2.1. Controllers at T_A^c, T_B^c and T_C^c

The three controllers are on the cooling side. The controller T_A^{c} is set at $T_{\mathrm{s}} = 14.5$ °C, $\Delta T = 2.0$ °C and T_B^{c} at $T_{\mathrm{s}} = 14.5$ °C, $\Delta T = 2.5$ °C. Controller T_C^{c} is set at $T_{\mathrm{s}} = 14.5$ °C with variable dead-band 0.4 °C < ΔT < 4 °C.

The effect of the dead-band on the three phase differences is shown in Fig. 8. For each dead-band, the network response is obtained for 15 min. The phase differences are shown as a series of plots; each corresponds to a fixed ΔT but the initial phase differences are subtracted out so that they all start from zero. In (a), the dead-bands of the two controllers T_A^{c} and T_B^{c} are close enough for synchrony, while T_C^{c} is not. With an increase in ΔT, they all slowly become asynchronous as shown in (c). On further increase all three oscillators synchronize, as in (f). After that, they are out of synchrony, as in (g). Finally, the dead-band becomes too large and the oscillation of T_C^{c} is out of synchrony with the others.

The three loop temperatures, $T_A^{\mathrm{c}}(t)$, $T_B^{\mathrm{c}}(t)$ and $T_C^{\mathrm{c}}(t)$, can be plotted in a phase space as shown in Fig. 9(a) and (b) (where they correspond to the signals in Fig. 8(d) and (f), respectively). Clearly, there is no synchronization in (a). In (b), synchronization introduces a "hole" in the plot and all three variables oscillate at similar frequencies; the phases of the three temperatures remain locked, while the amplitudes of the individual temperatures evolve independently. The flow in phase space is not exactly repeatable; this could be due to noise in the measured signals, nonlinearity in the system, or variations in the building chilled-water temperature.

3.2.2. Controllers at T_A^h, T_B^c and T_C^c

This a case where there is coupling between the heating and cooling sides. The controller for T_B^{c} is fixed at $T_{\mathrm{s}} = 16.5$ °C, $\Delta T = 2.5$ °C, while that for T_C^{c} is fixed at $T_{\mathrm{s}} = 16.5$ °C, $\Delta T = 4.5$ °C. The controller for T_A^{h}, on the other hand, has $T_{\mathrm{s}} = 18.5$ °C and variable dead-band 0.4 °C < ΔT < 4 °C.

The results of the phase differences are shown in Fig. 10. In the beginning the frequency detuning of the three oscillators is so large that they fail to synchronize, as shown in (b). As the dead-band grows the detuning becomes smaller and there is synchronization; ϕ_{AB} is nearly constant while the other two increase indefinitely as shown in (d). On further increasing the dead-band, ϕ_{AB} decreases indefinitely, though slowly, as in (e), but ϕ_{AC} becomes smaller. Now the two oscillators T_A^{h} and T_C^{c} begin to synchronize. After (f), the three oscillators are out of synchrony again.

4. Conclusions

Large-scale, complex thermal-hydraulic networks are sometimes broken up into sub-systems which are then designed independently and without regard to dynamic interaction between them. It is possible, however, that their dynamics may become coupled during operation. This may happen not only for identical sub-systems but also for those with slight dissimilarities. Here we have experimentally demonstrated the phenomenon of synchronization for a small-scale network. Self-sustained oscillations are generated by using thermostatic temperature control. Detuning between controllers has been varied by changing their dead-bands. With this the network has been observed in various states of synchronization. The phenomena of frequency- and phase-locking as well as phase slip were observed.

Though much more work needs to be done to generalize the results, this study may be helpful in the design of control systems for thermal-hydraulic networks. In building systems, for instance, it would be of concern if temperatures fluctuations in different areas were to enter into synchrony.

Acknowledgements

We acknowledge the support provided by the late Mr. D.K. Dorini of BRDG-TNDR for the first author and

the Hydronics Laboratory. We are also grateful for discussion on synchronization with Drs. Walfre Franco and Fredrik Carlsson.

References

[1] N. Wiener, Nonlinear Problems in Random Theory, MIT Press, Cambridge, MA, 1958.
[2] A.T. Winfree, The Geometry of Biological Time, Springer, New York, 1980.
[3] Y. Kuramoto, Chemical Oscillations, Waves, and Turbulence, Springer, New York, 1984.
[4] P.C. Matthews, S.H. Strogatz, Phase diagram for the collective behavior of limit-cycle oscillators, Phys. Rev. Lett. 65 (14) (1990) 1701–1704.
[5] M.K.S. Yeung, S.H. Strogatz, Time delay in the Kuramoto model of coupled oscillators, Phys. Rev. Lett. 82 (3) (1999) 648–651.
[6] A. Pikovsky, M. Rosenblum, J. Kurths, Synchronization: A Universal Concept in Nonlinear Sciences, Cambridge University Press, Cambridge, 2001.
[7] S.H. Strogatz, Sync: The Emerging Science of Spontaneous Order, Theia, New York, 2003.
[8] M. Rosenblum, A. Pikovsky, Synchronization: from pendulum clocks to chaotic lasers and chemical oscillators, Contemp. Phys. 44 (5) (2003) 401–416.
[9] C. Graves, L. Glass, D. Laporta, R. Melocha, A. Grassino, Respiratory phase locking during mechanical ventilation in anesthetized human subjects, Am. J. Physiol. 250 (1986) R902–R909.
[10] R.C. Elson, A.I. Selverston, R. Huerta, N.F. Rulkov, M.I. Rabinovich, H.D.I. Abarbanel, Synchronous behavior of two coupled biological neurons, Phys. Rev. Lett. 81 (25) (1998) 5692–5695.
[11] C. Schäfer, M.G. Rosenblum, H.H. Abel, J. Kurths, Synchronization in the human cardiorespiratory system, Phys. Rev. E 60 (1) (1999) 857–870.
[12] M. Nomura, T. Aoyagia, T. Fukai, Gamma frequency synchronization in a local cortical network model, Neurocomputing 50–60 (2004) 159–164.
[13] S.H. Strogatz, I. Stewart, Coupled oscillators and biological synchronization, Sci. Am. 269 (6) (1993) 102–109.
[14] D. Gonze, S. Bernard, C. Waltermann, A. Kramer, H. Herzel, Spontaneous synchronization of coupled circadian oscillators, Biophys. J. 89 (1) (2005) 120–129.
[15] I.Z. Kiss, Y.M. Zhai, J.L. Hudson, Emerging coherence in a population of chemical oscillators, Science 296 (5573) (2002) 1676–1678.
[16] E.S. Kurkina, E.D. Kuretova, Numerical analysis of the synchronization of coupled chemical oscillators, Comput. Math. Model. 15 (1) (2004) 38–51.
[17] M.S. Wang, Z.H. Hou, H.W. Xin, Internal noise-enhanced phase synchronization of coupled chemical chaotic oscillators, J. Phys. A—Math. Gen. 38 (1) (2005) 145–152.
[18] Y. Zhang, G.H. Du, Spatio-temporal synchronization of coupled parametrically excited pendulum arrays, J. Sound Vib. 239 (5) (2001) 983–994.
[19] M. Bennett, M.F. Schatz, H. Rockwood, K. Wiesenfeld, Huygens's clocks, Proc. R. Soc. London Ser. A—Math. Phys. Eng. Sci. 458 (2002) 563–579.
[20] A. Vilfan, T. Duke, Synchronization of active mechanical oscillators by an inertial load, Phy. Rev. Lett. 91 (11) (2003). Article No. 114101.
[21] A. Fradkov, B. Andrievsky, K. Boykov, Control of the coupled double pendulums system, Mechatronics 15 (10) (2005) 1289–1303.
[22] S. Banerjee, P. Saha, A.R. Chowdhury, On the application of adaptive control and phase synchronization in non-linear fluid dynamics, Int. J. Non-Linear Mech. 39 (1) (2004) 25–31.
[23] K. Wiesenfeld, P. Colet, S.H. Strogatz, Frequency locking in Josephson arrays: connection with the Kuramoto model, Phys. Rev. E 57 (2) (1998) 1563–1569.
[24] I.A. Heisler, T. Braun, Y. Zhang, G. Hu, H.A. Cerdeira, Experimental investigation of partial synchronization in coupled chaotic oscillators, Chaos 13 (1) (2003) 185–194.
[25] S. Cincotti, S. Di Stefano, Complex dynamical behaviours in two non-linearly coupled Chua's circuits, Chaos Soliton. Fract. 21 (3) (2004) 633–641.
[26] L.M. Pecora, T.L. Carroll, Synchronization in chaotic systems, Phys. Rev. Lett. 64 (8) (1990) 821–823.
[27] A.S. Pikovsky, M.G. Rosenblum, J. Kurths, Synchronization in a population of globally coupled chaotic oscillators, Europhys. Lett. 34 (3) (1996) 165–170.
[28] M.G. Rosenblum, A.S. Pikovsky, J. Kurths, Phase synchronization of chaotic oscillators, Phys. Rev. Lett. 76 (11) (1996) 1804–1807.
[29] M.G. Rosenblum, A.S. Pikovsky, J. Kurths, Phase synchronization in driven and coupled chaotic oscillators, IEEE Trans. Circuits Systems I—Fundam. Theory Appl. 44 (1997) 874–881.
[30] M.G. Rosenblum, A.S. Pikovsky, J. Kurths, From phase to lag synchronization in coupled chaotic oscillators, Phys. Rev. Lett. 76 (11) (1997) 4193–4196.
[31] G.V. Osipov, A.S. Pikovsky, J. Kurths, Phase synchronization of chaotic rotators, Phys. Rev. Lett. 88 (5) (2002). Article No. 054102.
[32] S. Boccaletti, J. Kurths, G. Osipov, D.L. Valladares, C.S. Zhou, The synchronization of chaotic systems, Phys. Rep. 366 (2002) 1–101.
[33] I. Leyva, E. Allaria, S. Boccaletti, F.T. Arecchi, In phase and antiphase synchronization of coupled homoclinic chaotic oscillators, Chaos 14 (1) (2004) 118–122.
[34] S. Boccaletti, E. Allaria, R. Meucci, Experimental control of coherence of a chaotic oscillator, Phys. Rev. E 69 (6) (2004). Article No. 066211, Part 2.
[35] H. Fotsin, S. Bowong, Adaptive control and synchronization of chaotic systems consisting of Van der Pol oscillators coupled to linear oscillators, Chaos Soliton. Fract. 27 (3) (2006) 822–835.
[36] X. Gao, J.B. Yu, Synchronization of two coupled fractional-order chaotic oscillators, Chaos Soliton. Fract. 26 (1) (2005) 141–145.
[37] G.Y. Han, A mathematical model for the thermal-hydraulic analysis of nuclear power plants, Int. Commun. Heat Mass Transfer 27 (6) (2000) 795–805.
[38] E. Erell, Y. Etzion, Heating experiments with a radiative cooling system, Build. Environ. 31 (6) (1996) 509–517.
[39] S.H. Cho, M. Zaheer-Uddin, An experimental study of multiple parameter switching control for radiant floor heating systems, Energy 24 (5) (1999) 433–444.
[40] R.D. Judkoff, J.S. Neymark, A procedure for testing the ability of whole building energy simulation programs to thermally model the building fabric, ASME J. Solar Energy Eng. 117 (1) (1995) 7–15.
[41] I.E. Lane, N. Beute, A model of the domestic hot water load, IEEE Trans. Power Syst. 11 (4) (1996) 1850–1855.
[42] K.J. Graviss, R.L. Collins, Control of household refrigerators Part I: modeling temperature control performance, HVAC & R Res. 4 (4) (1998) 427–443.
[43] B. Cahlon, D. Schmidt, M. Shillor, X. Zou, Analysis of thermostat models, Eur. J. Appl. Math. 8 (1997) 437–455.
[44] X. Zou, J.A. Jordan, M. Shillor, A dynamic model for a thermostat, J. Eng. Math. 36 (4) (1999) 291–310.
[45] C.Y.S. Hung, H.N. Lam, A. Dunn, Dynamic performance of an electronic zone air temperature control loop in a typical variable-air-volume air conditioning system, HVAC & R Res. 5 (4) (1999) 317–337.
[46] W.G. Chun, M.S. Jeon, Y.S. Lee, H.S. Jeon, T.K. Lee, A thermal analysis of a radiant floor heating system using SERI-RES, Int. J. Energy Res. 23 (4) (1999) 335–343.
[47] J.C. Chipman, W. Houtz, M. Shillor, Simulations of a thermostat model I: approach to steady states, Math. Comput. Modell. 32 (7–8) (2000) 765–790.
[48] N. Lu, D.P. Chassin, A state-queueing model of thermostatically controlled appliances, IEEE Trans. Power Syst. 19 (3) (2004) 1666–1673.

[49] M.S. Liu, J.R. Wang, Energy performance analysis of coupled-control units with both thermostat and humidistat, ASME J. Solar Energy Eng. 127 (1) (2005) 65–69.
[50] W. Franco, Hydrodynamics and Control in Thermal-fluid Networks, Ph.D. dissertation, Department of Aerospace and Mechanical Engineering, University of Notre Dame, Notre Dame, IN, 2003.
[51] W. Franco, M. Sen, K.T. Yang, R.L. McClain, Dynamics of thermal-hydraulic network control strategies, Exp. Heat Transfer 17 (2004) 161–179.
[52] W. Franco, M. Sen, K.T. Yang, R.L. McClain, Comparison of thermal-hydraulic network control strategies, Proc. Inst. Mech. Eng. Part I: J. Syst. Control Eng. 217 (2003) 35–47.
[53] W. Cai, W. Franco, G. Arimany, M. Sen, K.T. Yang, R.L. McClain, Interaction between secondaries in a thermal-hydraulic network, ASME J. Dyn. Syst., Meas. Control, in press.
[54] J.K. Hammond, P.R. White, The analysis of non-stationary signals using time–frequency methods, J. Sound Vib. 190 (3) (1996) 419–447.
[55] S.H. Strogatz, R.E. Mirollo, Collective synchronization in lattices of nonlinear oscillators with randomness, J. Phys. A (Math. Gen.) 21 (13) (1988) L699–L705.
[56] Z. Zheng, G. Hu, B. Hu, Phase slips and phase synchronization of coupled oscillators, Phys. Rev. Lett. 81 (24) (1998) 5318–5321.